Article:
Farshchi, A, Hassanpour, A, Tantawy, H et al. (2022) Effect of matrix composition on the flowability of spray-dried detergent powders. Advanced Powder Technology, 33 (3). 103433. ISSN: 0921-8831

https://doi.org/10.1016/j.apt.2022.103433

Effect of matrix composition on the flowability of spray-dried detergent powders

Amin Farshchi[1,2*], Ali Hassanpour[2], Hossam Tantawy[3], Andrew E. Bayly[2*]

[1]*School of Health and Life Sciences, Teesside University, Middlesbrough, TS1 3BX, UK*

[2]*School of Chemical and Process Engineering, University of Leeds, Leeds, LS2 9JT, UK*

[3]*The Procter & Gamble Company, Newcastle Innovation Centre, Newcastle-Upon-Tyne NE12 9TS, United Kingdom*

* Corresponding authors.

Amin Farshchi, E-mail: a.farshchi@tees.ac.uk

Andrew E. Bayly, E-mail: a.e.bayly@leeds.ac.uk

Introduction

Spray drying is a common process for manufacturing many granular products such as food powders, detergents, and pharmaceuticals. The flow characteristics of these powders play an important role in subsequent handling and processing operations, *e.g*. feeding, mixing and compaction. Typically, well-formulated products are free flowing, this ensures a reliable and consistent feed from hoppers and feeders into downstream processes (Muir, 2007). Occasionally, some formulations can be cohesive, causing issues with the discharge from silos and hoppers; arching and ratholing may occur in the worst-case scenarios, which can result in the stoppage of the process. These flow problems are mainly governed by physicochemical properties of powders which include particle size and morphology, particle size distribution, surface micro-structure and moisture content (Barjat et al., 2020, Schubert, 1987). The mechanical properties of the powder are also important to flowability (Thomas, 2004). Although a great deal of work has been reported in the literature on the flowability of many powders, there has been limited work on the flowability of spray dried powders, in general, and no work on the flowability of spray-dried detergent powders and how it is influenced by the slurry formulation, at least in the public literature.

Laundry detergent powder is a multi-component solid predominantly consisting of a surfactant, which comprises up to 50% by weight of the detergent, and other specific materials, *e.g*. builders, bleaches, and fillers. A wide variety of different detergent brands and types are manufactured across the world. Spray drying is the most prevalent process for the manufacture of laundry detergent powders. In this process a slurry formed from a mixture of liquid and powder ingredients is transformed into a dry powder, also referred to as “blown powders”. Blown powders commonly contain thermally stable and chemically compatible ingredients, *e.g*. surfactant, fillers and builders, and comprise 30-90 wt% of the finished detergent powders (Boerefijn et al., 2007, Zoller and Sosis, 2008). The sodium salt of linear

alkylbenzene sulphonate (NaLAS), also known as LAS paste, is a key component of typical detergent formulations and is a key factor controlling product physical properties and many performance related characteristics e.g. dissolution rate, caking tendency.

A detergent slurry typically consists of a continuous aqueous phase supersaturated with respect to inorganic salts, in which liquid crystalline phases of surfactant molecules along with undissolved inorganic salts and binders are suspended. Upon drying, aqueous and liquid crystalline phases are transformed into a porous solid matrix consisting of partially-dehydrated liquid crystalline phases of surfactants as well as nano-sized crystals of inorganic salts (Farshchi et al., 2021). It was previously shown that the initial water content of the slurries plays a crucial role in the matrix composition and micro-structure of the resulting powders. The greater the slurry water content, the greater the proportion of sodium sulphate that is dissolved in the slurry (Farshchi et al., 2019a). This consequently increases the ratio of inorganic salts to NaLAS within the dried matrix phase of the powders. Binders *e.g.* sodium silicate, polycarboxylates are typically required to improve the mechanical properties of the powders. Sodium silicate is a common binder, which acts as a builder augmenting the detergency performance of the formulation, as well as providing reinforcement to the matrix, and hence the structure of the surfactant based powders (Keeley, 1983). Concentrated sodium silicate solutions are alkaline colloidal dispersions of silicate anion species, and characterized by a SiO_2:Na_2O molar ratio, which lies in the range of 1.6 to 3.8. Varying the molar ratio gives rise to solutions having different characteristics, *e.g.* rheological and binding characteristics (Roggendorf et al., 2001, Tognonvi et al., 2010, Yang et al., 2008).

Therefore, from the technological point of view, the matrix micro-structure changed by either varying the SiO_2:Na_2O or the initial water content of the slurries, may have a significant impact on the particle robustness and consequently powder flow behaviour.

The focus of the current work will be on demonstrating that the matrix composition, which is also reflected on the particle surface, is a key parameter influencing the bulk properties of spray-dried detergent powders, *e.g.* flowability, tapped density and compressibility. In this study, the role of water as a key ingredient of the detergent slurry, which governs the matrix composition, is particularly highlighted. The effect of slurry formulation on the morphology, surface texture, and surface chemical composition of the particles was probed by a combination of confocal Raman microscopy, Morphologi G3, and scanning electron microscopy (SEM) techniques. The flow characteristics were evaluated using shear testing techniques and by measuring the bulk and tapped densities, which are some of the common techniques used to provide numerical scales for powder flow properties.

2. Material and methods

2.1. Materials

Four model formulations of detergent granules were produced with a pilot-scale spray dryer by Procter & Gamble. Typical production process conditions were used, and these were kept consistent between formulations. Detergent slurries with a temperature of 85°C were introduced into the spray dryer operating under the following conditions: inlet air temperature 280°C, exhaust temperature 100°C. Further information on operating conditions can be found in (Farshchi et al., 2019a). All spray-dried powders contained the sodium salt of LAS, with a molecular weight of 340 g/mol, and sodium sulphate. However, their formulation varied depending on either the initial water content (30.0 or 63.0 wt%) of the slurry or the addition of sodium silicate with molar-ratios of 1.6 and 2.35 SiO_2:Na_2O. These compositions are shown in Table 1. The abbreviations used to identify the formulations are used throughout this paper: **LW**: low-water content slurry; **HW**: high-water content slurry; **LW + 1.6R** and

LW + 2.35R: low-water content slurry containing sodium silicate with the SiO_2:Na_2O molar ratios of 1.6 and 2.35 respectively.

Table 1. Composition of the detergent slurry formulations

	Compositions of the detergent slurries (wt %)				
Description	Water	LAS	Sodium sulphate	Sodium silicate (1.6R)	Sodium silicate (2.35R)
LW	30.0	13.6	56.4		
HW	63.0	7.2	29.8		
LW + 1.6R	28.0	14.0	49.3	8.6	
LW + 2.35R	28.0	14.0	47.2		10.8

Notes: (LW) low-water content slurry; (HW) high-water content slurry; (LW+1.6R) low-water content slurry containing 1.6 SiO_2:Na_2O R; and (LW+2.35R) low-water content slurry containing 2.35 SiO_2:Na_2O R; (LAS) linear alkylbenzene sulphonate.

Although, the LW and HW slurry formulations differ in initial water content, the resulting detergent powders will have identical chemical composition: 19.5 wt% NaLAS, 0.5 – 1.0 wt % water, 80.5 – 81.0 wt% sodium sulphate; however, their micro-structure and matrix composition is significantly different. The matrix phase is defined as the solid continuous phase, excluding the sodium sulphate particles which were undissolved in the slurry, in which nano-sized crystals of inorganic salts along with lamellar liquid crystalline phases of LAS are dispersed. For the LW formulation the mass ratio of sodium sulphate to NaLAS within the matrix phase, is considerably lower than that ratio in the HW formulation, due to the lower solubility of sodium sulphate in 30 wt% water (Farshchi et al., 2019a). The formation of

compositionally different surface micro-structure as a result of the formation of different matrix phases will be discussed later in section 3.3. Particle size distribution are known to play a key role in the flowability of powder, therefore, prior to tapped density and flowability measurements the powders were sieved using a sieve shaker and a fraction of 300-350 μm was selected for the analysis. This diminishes the influence of particle-particle adhesion forces, *e.g*. van der Waals forces, which become more pronounced compared with gravity forces, with decreasing the particle size. It was also previously demonstrated that silicate containing detergent powders show a considerable increase in moisture uptake above 40% RH, which was attributed to the hygroscopic nature of sodium silicates (Farshchi et al., 2019b). Therefore, prior to flowability and mechanical strength measurements, the sieve cuts (300-350 μm) of the spray-dried powders were conditioned in desiccators with a specific relative humidity of 33% at 21±1°C for 48h. This specific relative humidity was created using a saturated solution of magnesium chloride.

2.2. Morphology analysis

The morphologies of the sieve cuts, *i.e*. 300-350 μm, of the detergent powders were evaluated using a scanning electron microscope (HITACHI Benchtop TM3030 Plus). Prior to loading in the SEM, the samples were sputter coated with an ultra-thin coating of gold to inhibit charging during SEM examination. The shape analysis of the sieve fractions was carried out using an image-based system, the Malvern Morphologi G3 (Malvern Instrument, Malvern UK). The Malvern Morphologi G3 is an automated image analysis system which captures two dimensional (2D) image of a 3D particle and calculates several parameters of the size and shape of the particle. Particle imaging was carried out using 5× magnification lens (6.4 μm – 420 μm). The characteristic morphological parameters which the Morphologi software uses to describe shapes were High Sensitivity Circularity (*HSC*), Convexity,

Elongation and Aspect ratio. Definitions of the morphological parameters can be found in (Gamble et al., 2014, Ulusoy and Kursun, 2011).

2.3. Flow properties

The flow behaviour of the resulting spray-dried detergent powders was investigated using a ring shear cell tester (Schulze RST-XS, Wolfenbüttel, Germany). For the flowability measurement, the powder was loosely loaded into the annular shear cell. After loading, the specimen was pre-sheared under a pre-sheared normal stress, σ_{pre}, *e.g.* 2.0, 4.0, 6.0 and 8.0 kPa, until a steady-state flow is achieved (shear stress remains constant). The second step of the test is shear to failure point, *i.e.* unconfined yield strength, σ_c. In this stage the critically consolidated specimens are sheared to failure under a normal stress, σ_{sh}, which is less than the initially applied normal stress, σ_{pre}, causing particles to move against each other. During shear testing the shear cell rotates, whereas the lid is prevented from rotation. Therefore, a shear deformation is created within the bulk powder and the required torque is measured and converted into a shear stress, τ_{sh}, and consequently a point of incipient flow is measured, and yield locus is constructed based on the individual shear points (σ_{sh}, τ_{sh}) by completing the procedure of consolidation and shearing under different levels of normal stress. The yield locus and a Mohr stress circle which is tangential to the yield locus and intersects at the point of steady state flow (σ_{sh}, τ_{sh}), are used to determine the parameters describing the flow behaviour of bulk solids. The detailed procedure has been described by Schulze (2007). These parameters include cohesion coefficient, τ_c, angle of internal friction at incipient flow, φ_{lin}, effective angle of internal friction, φ_e, and flow index, ff_c. The cohesion coefficient, τ_c, describes cohesion between particles in a solid bulk (Poszytek, 2005). The friction angles are related to the friction between particles. A flow function plot can be generated by plotting the unconfined yield stress, σ_c, versus major consolidation stress, σ_1, of the corresponding yield

locus. The inverse of the slope of the line gives a flow index, ff_c, which is used to describe the flowability of a powder according to Jenikes's classification (Jenike, 1967).

The flowability of spray-dried powders was also evaluated by Hausner ratio. The ratio of the tapped bulk density, ρ_{tapped}, to its initial bulk density, $\rho_{initial}$, is known as Hausner ratio which can be expressed as:

$$HR = \frac{\rho_{tapped}}{\rho_{initial}} \qquad (1)$$

The loose bulk density was determined by pouring a known weight of the sample in a 50 ml graduated cylinder, through a funnel which was positioned at a certain height. The tapped density was obtained by tapping the cylinder using a Tapped Density Tester (Series JV 2000; Copley Scientific Limited, Nottingham, UK) after 1250 taps (Fitzpatrick et al., 2004b), until no further change in the powder volume was observed. In general, a free-flowing powder is less effected by tapping. Therefore, a lower Haunser ratio of a powder indicates a better flow characteristic (Liu et al., 2008). Hayes (1987) classified the flow behaviour of bulk solids according to their Hausner ratio (HR), as can be seen in Table 2.

Table 2. Hayes's classification of powder flowability by Hausner ratio (*HR*).

Flowability	Very difficult flowing	Difficult flowing	Medium flowing	Free flowing
Hausner ratio (*HR*)	HR> 1.4	1.25<HR<1.4	1.1<HR<1.25	1<HR<1.1

2.4. Micro-computed tomography (Micro-CT) scanning

In the present work, interstitial spaces between the granules, as a measure of packing density, were qualitatively examined using a Phoenix Nanotom CT scanner (GE Measurement and Control, Wunstorf, Germany). Detergent powders were loaded in a plastic tube (internal diameter 2 mm, height 8.5 mm). After manually tapping on a flat surface, the plastic tube was mounted on a rotating stage between an X-ray source and X-ray detector. Samples were then scanned in the full range of 0–360°. A series of X-ray micrographs were obtained, and three-dimensional volumes were reconstituted using a VGStudio software package (Volume Graphics GmbH, Heidelberg, Germany). The original volume was cropped and a cube (1500×1500×1500 μm) was created for further image processing (Fig. 1b). To improve the 3D data visualisation, a number of different image processing tools, including filtration and segmentation, were applied to the X-ray micrograph data using Avizo software package 8.0 (FEI, Oregon, USA). Prior to the segmentation process, a non-local mean filtration was applied to the grey scale projection to reduce image noise. The segmentation was conducted using an interactive thresholding tool in Avizo.

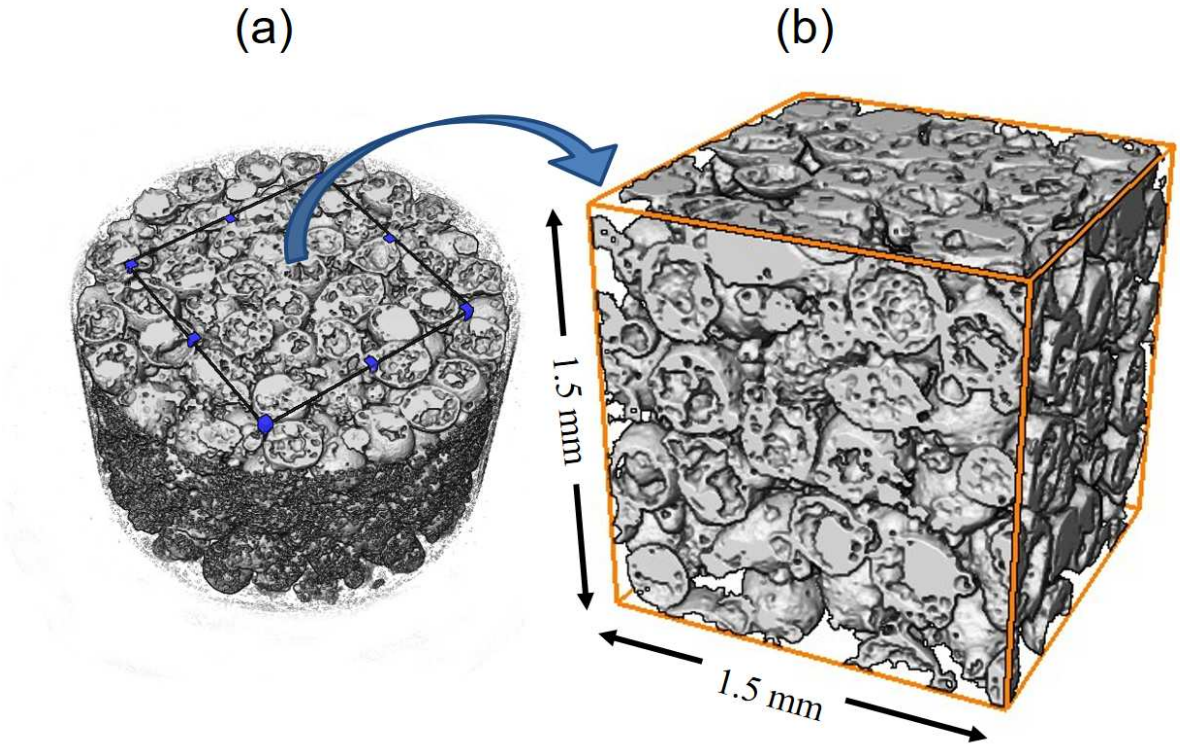

Figure. 1. (a) 3D X-ray tomograph (voxel size: 2.56×2.56×2.56 μm) from a cross-section of a plastic tube loaded with detergent granules, showing the region of interest. (b) A cube (1.5×1.5×1.5 mm) cropped from the original volume for the qualitative analysis of packing density.

2.5. Raman microspectroscopic analysis

Confocal Raman microscopy was used to probe the surface composition of the detergent granules. All Raman spectra were obtained using an inVia confocal Raman microscope (Renishaw plc, New Mills, UK) equipped with 514 nm helium–neon laser excitation. A 50× objective lens was used, giving a laser spot diameter of 2 μm. The spectra were obtained from a 30 sec exposure using a CCD detector in the region 400-3200 cm^{-1} and the extended scanning mode of the instrument. Post-processing and data analysis were carried out with Renishaw WiRE 3.3 and Origin software. Laser-induced fluorescence which is frequently encountered in specimens containing organic compounds, results in baseline drifts distorting the spectrum towards the end. The sloping enhanced backgrounds were subtracted with a fifth-order polynomial (Marshall and Olcott Marshall, 2013).

2.6. Mechanical strength measurements

2.6.1. Single particle compression test

Compression tests were performed using an Instron Universal Testing Machine (Model 5566, Instron Crop., USA). For single particle compression test, 20-25 granules were compressed individually between two rigid platens in the axial direction at a slow rate of 0.5 mm/min. The compression was performed using a 10 N load cell which had a resolution of 0.25 mN. The detergent granules were subjected to a maximum compressive load of 0.05 N. The compression force was measured using a 10 N load cell transducer and, the axial load and the machine head displacement were continuously recorded by the system's computer. The force-

displacement curves obtained from the compression tests were then evaluated to calculate the granule rupture strength, σ_r, Eq. (2) (Samimi et al., 2005).

$$\sigma_r = \frac{4F_r}{\pi D^2} \qquad (2)$$

Where F_r is the rupture force and D is the diameter of the granule. The parameter D was determined by measuring the diametrical distance between two rigid platens as first contact between the moving platen and surface of the granules was identified through the force-displacement curves. The rupture force can be determined manually from the peak failure force in force-displacement curves, where the first sharp decrease in loading force can be observed (Fig. 2).

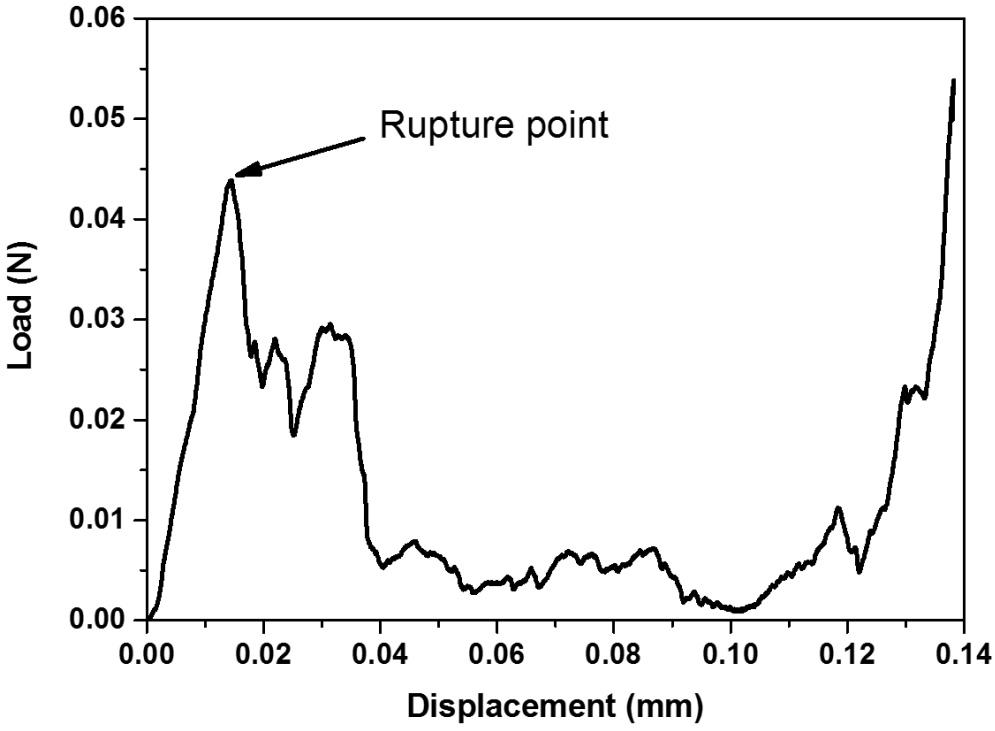

Figure. 2. Typical force-displacement curve obtained from the single granule compression test.

2.6.2. Bulk compression test

Bulk compression tests were carried out using the same Instron machine. A known mass of the sample was poured into a cylindrical die with a height and diameter of 20 mm and tapped until the volume did not decrease any further. The sample was then compressed with a close-fitting stainless-steel piston until the maximum compaction force of 120 N was reached. This compressive force ensures that all samples will develop a linear relationship between the applied pressure and the volume reduction of a powder bed being compacted, which is required for yield strength measurements using the Kawakita model. This empirical equation was proposed by (Kawakita and Lüdde, 1971) for analysis of soft and fluffy powders, which expresses the relationship between volume and applied pressure during compression, Eq. (3).

$$\frac{P}{C} = \frac{1}{ab} + \frac{P}{a} \qquad (3)$$

Where C is the degree of volume reduction or engineering strain, and calculated as $C=(V_0-V)/V_0$, where V_0 is the initial powder bed volume and V is the powder volume at pressure P. The parameters a and b are the Kawakita constants. The parameter a is related to the initial bed porosity and mathematically describes the degree of compression at infinite pressure. The parameter b is related to the resistance force. The term 1/b describes the applied pressure required to compress the powder to one-half the maximum degree of compression or $a/2$. The parameter $1/b$ has been shown to be related to the yield strength and plasticity of the materials (Khomane et al., 2013). The Kawakita profiles can be obtained by plotting the experimental values of P/C as a function of P. The compression parameters were then determined by linear regression analysis of the profiles, in the pressure range of 250-375 kPa.

2.7. Statistical analysis of the data

The results of single particle compression test were subjected to one-way analysis of variance (ANOVA) for the comparison of mean values of granule strength, and the significance of differences among the testing formulations was analysed by post-hoc Tukey's HSD ("honestly significant differences") at $P < 0.05$ significant level, 95% confidence limit. The statistical analysis was performed using IBM SPSS 20 (IBM Corp. IBM SPSS Statistics for Windows, version 20.0. Armonk, NY: IBM Corp.).

3. Results and discussion

3.1. Morphology analysis

The morphological characteristics of the detergent powders can be seen in Fig. 3. The granules produced from low-water content slurries (LW) are almost spherical, though in the presence of sodium silicate, a small number of fine particles can be observed adhered to the surface of primary particle. The most outstanding, morphological characteristic can be seen in HW formulations where the detergent granules show a greater degree of agglomeration, and blistering. The reasons for these morphological properties were discussed in previous work (Farshchi et al., 2019a).

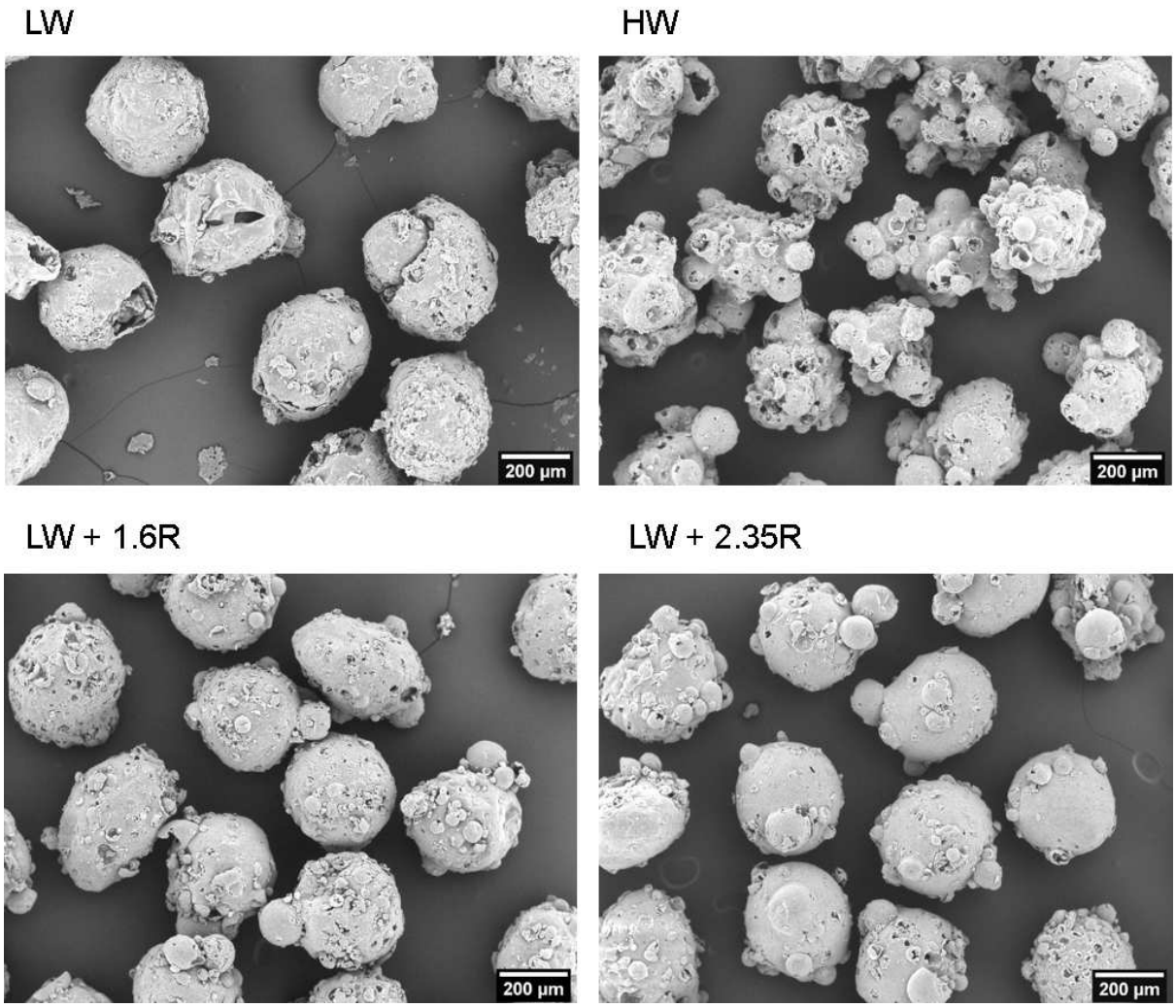

Figure 3. SEM micrographs of spray dried detergent powders (300-350 µm).

The morphological properties observed in SEM micrographs were also statistically reflected in the particle shape analysis carried out using the Malvern Morphologi G3, in which high sensitivity circularity, convexity, aspect ratio and elongation were chosen as shape parameters (Table 3). Convexity is a measure of edge roughness. It can be seen that LW formulation shows the largest convexity value, 0.950. However, the convexity value decreases to 0.931 and 0.927 on addition of sodium silicate with the SiO_2:Na_2O molar ratios of 1.6 and 2.35 respectively, which is probably due to some surface agglomeration. For the HW formulations the puffing and agglomeration are more noticeable, resulting in the lowest convexity value, 0.887. Amongst the shape parameters, HSC is sensitive to both changes in

overall shape and edge roughness. Comparing the HSC values, once again, the HW formulations were found to be more irregular in shape with rougher outlines.

Table 3. Mean values for the shape characteristics of spray-dried detergent powders determined by Malvern Morphologi G3.

Powder sample	HS Circularity	Convexity	Elongation	Aspect ratio
LW	0.815	0.950	0.174	0.826
HW	0.652	0.887	0.185	0.815
LW + 1.6R	0.774	0.931	0.136	0.864
LW + 3.35R	0.757	0.927	0.142	0.858

3. 2. Flowability measurements

The measured flow functions of spray-dried detergent powders are shown in Fig. 4a. The flow index of each sample was determined from the slope of the flow function which has been summarised in the figure. In general, a steep slope of the flow function represents a cohesive powder with poor flow characteristics. For detergent powders produced from low-water content slurry without silicate (LW), the higher flow function gradient implies that the granules have developed a greater strength upon consolidation, which is then required to be overcome by a greater force to initiate flow (Fitzpatrick et al., 2004a). These samples showed the lowest flow index value and were classified as a very cohesive powder ($1 < ffc < 2$). Interestingly, when powders of the same formulation was made from a higher water content slurry (HW) the flow-behaviour improved significantly, though they are still classified as cohesive materials ($2 < ffc < 4$).

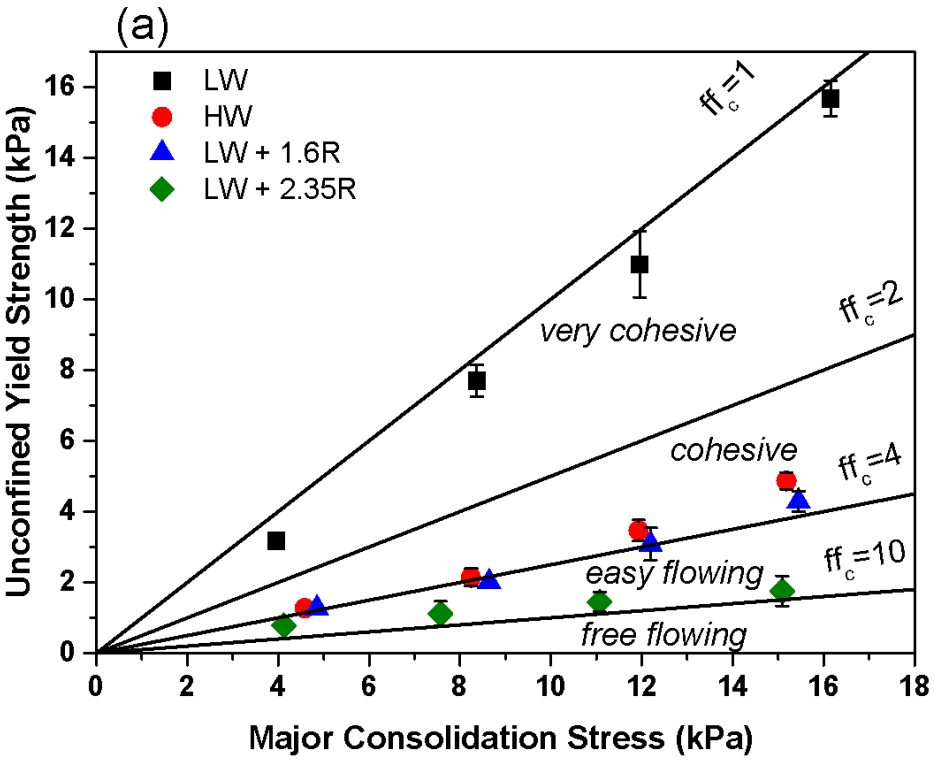
(a)
LW
HW
LW + 1.6R
LW + 2.35R
ff$_c$=1
ff$_c$=2
ff$_c$=4
ff$_c$=10
very cohesive
cohesive
easy flowing
free flowing
Unconfined Yield Strength (kPa)
Major Consolidation Stress (kPa)
0
2
4
6
8
10
12
14
16
18

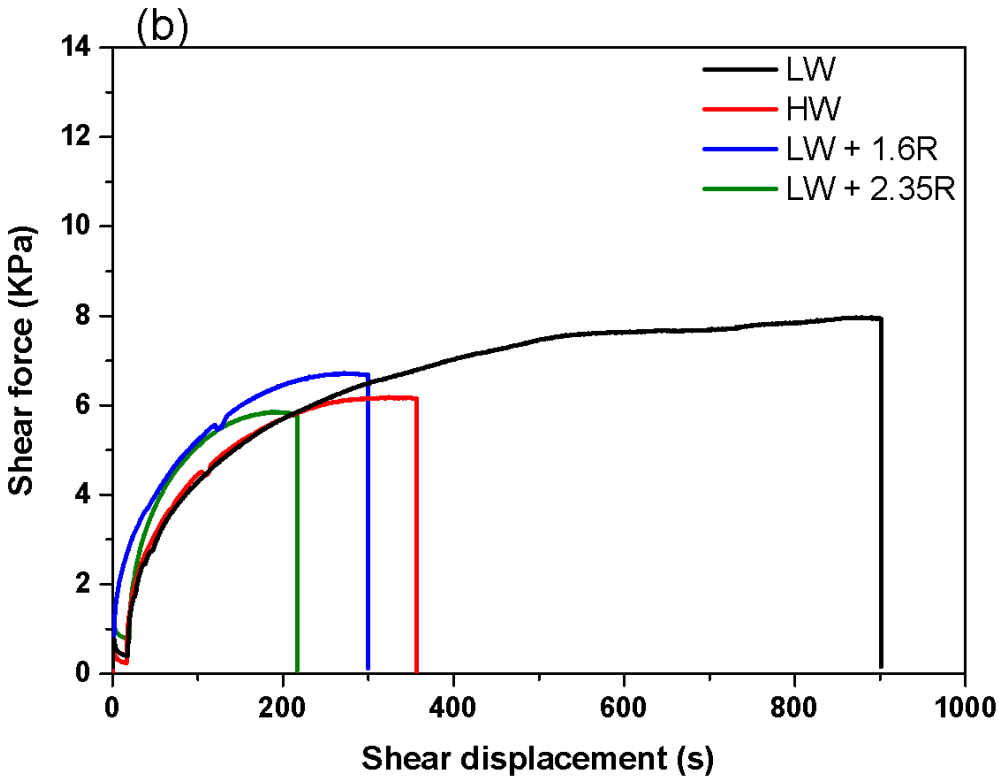
(b)
LW
HW
LW + 1.6R
LW + 2.35R
Shear force (KPa)
Shear displacement (s)
0
2
4
6
8
10
12
14
0
200
400
600
800
1000

Figure 4. Comparison of the flowability of spray-dried powders: (a) instantaneous flow functions of spray-dried detergent powders, (b) results of force-displacement obtained from the pre-shearing stages, measured at 8.0 kPa, σ_{pre}.

Returning to microscopic observations (Fig. 3) and shape analysis results in Table 3, it was shown that HW formulations were more irregular in shape. In general, granules with a rougher surface have a larger number of contacts which results in a greater frictional inter-particle interaction, *e.g*. mechanical interlocking, (Zhou and Qiu, 2010). Therefore, these results suggest that even though granule morphology can play a significant role in determining the flow properties, other factors might have been more predominant. A possible reason for the improved flowability of the irregular detergent granules can be explained by changes in matrix composition of these granules as a consequence of the increased water content of the slurries. This may consequently influence the granule structure and hence micro-properties, *e.g*. particle contact stiffness, of the powder, thereby affecting their macro-behaviour, *e.g*. flow-behaviour (Tomas, 2004a). The influence of initial water content of the slurries on the matrix composition as well as surface micro-structure of the powders will be discussed later in section 3.3.

The improved flowability, was also observed upon the addition of sodium silicates to the slurry formulations. For low-water content detergent slurries, the addition of sodium silicate with the SiO_2:Na_2O molar ratio of 1.6 slightly improved the flow behaviour from a very cohesive to cohesive character. However, the detergent powders were characterised as easy-flowing ($4 < ff_c < 10$) once the SiO_2:Na_2O molar ratio of sodium silicate was increased to 2.35.

The evaluation of consolidation behaviour of the powder beds during the pre-shearing stage of the flow measurement, provided some clues to the role of components as well as the matrix composition in the compressibility, and mechanical robustness of these powders. The

extent of compressibility is evident in Fig. 4b showing the shear force-displacement curves during pre-shearing stages of shear cell test measurements. At the pre-shearing stage, the powder bed may undergo a deformation whereby the granules rearrange themselves and fill the voids within the powder bed. As the bed deformation progresses by rearranging and sliding of the particles, as a consequence of the increasing normal stress, the bulk volume decreases due to the reduction of interstitial spaces. This gives rise to increasing the number of contacts between the particles, consequently developing shear forces within the powder bed. The build-up of shear force at this stage can also be accompanied by frictional plastic deformation *i.e*. flattening of the contact area, of the sheared particles until a constant shear force is reached. For easy-flowing powders, the powder bed reaches steady-state at a lower shear force than cohesive powders which take a longer period of time to reach the maximum force due to more prolonged particle deformation. (Hintz et al., 2008). The resulting shear force in these cohesive cases can be close to the magnitude of the applied normal stress.

From Fig. 4b it can be seen that for LW formulation, a relatively long time is required to obtain a constant shear rate. In other words, a large deformation within the powder bed is required to reach a steady-state flow. This implies a structurally loose powder bed, possibly due to the presence of many voids, *i.e*. interstitial spaces, which collapses with increasing the applied normal force. As mentioned earlier, the build-up of the shear force upon the reduction of the interstitial spaces, can occur in parallel with the plastic deformation. For very cohesive detergent powders (LW), a considerably prolonged shear-displacement after 500 s of pre-shearing can also be due to a frictional plastic deformation. (Tomas, 2004a) investigated the fundamentals of flow behaviour of cohesive powders, both theoretically and empirically, and showed a complete set of physically based equations for different states of powder flow, *e.g*. steady-state flow and incipient flow, during a shear test. The author suggested that the effect of surface micro-properties, *e.g*. surface contact stiffness or softness, on the flowability, can

be indirectly described from the angles of internal friction at steady-state, $\varphi_{e,}$ and incipient flows, φ_{lin}. The smaller the differences between these values, the stronger the particle contact points and, hence, the more free-flowing powder. The flow properties of spray-dried powders, at 8.0 KPa normal pressure, are shown in Table 4.

Table 4 Flow indices and friction angles, *i.e*. φ_{lin} and φ_e of spray-dried detergent powders measured under a pre-sheared normal stress of 8.0 kPa

Description	ff_c	φ_e	φ_{lin}
LW	1.03	76.6	21.6
HW	3.09	44.9	36.4
LW + 1.6R	3.40	43.4	35.3
LW + 2.35R	8.60	37.6	34.7

A relatively large difference can be seen (Table 4) between φ_e and φ_{lin} for the LW samples. This likely points to softer surface contacts between the detergent granules. From the analysis of the results of shear-cell test measurements, it can be inferred that very cohesive detergent powders, LW formulations, are likely to possess a structurally loose, and low-bulk density bed in which the detergent granules probably undergo a greater frictional plastic deformation with increasing the shear force. The greater the plastic deformation, the greater will be the cohesion of the contacts due to the increased surface area (Pasha et al., 2014). The influence of the matrix composition on the mechanical properties of the detergent granules will be discussed in section 3.4.

X-ray microtomography technique can provide good insight into the packing density of the granules within bulk solids. The 3D reconstructions of the regions of interest from the original volumes, plastic tubes, are illustrated in Fig. 5. Slightly larger interstitial spaces, *i.e*.

inter-particle voidage, can be seen for the powders produced from low-water content slurries (LW). This XRT observation is in good agreement with the results of tapped density measurements obtained from the Tapped Density Tester, which suggest that LW formulations have a tendency to form a structurally loose powder bed with many interstitial spaces upon pouring in a container, which subsequently undergo a greater degree of particle rearrangement upon tapping (Li et al., 2004, Nordström and Alderborn, 2011). In general, the greater the compressibility, the poorer is the flowability. LW formulations showed a relatively larger Hausner ratio (HR=1.14), as compared with other samples, which are considered to be medium flowing according to the classification of Hayes (Table 2).

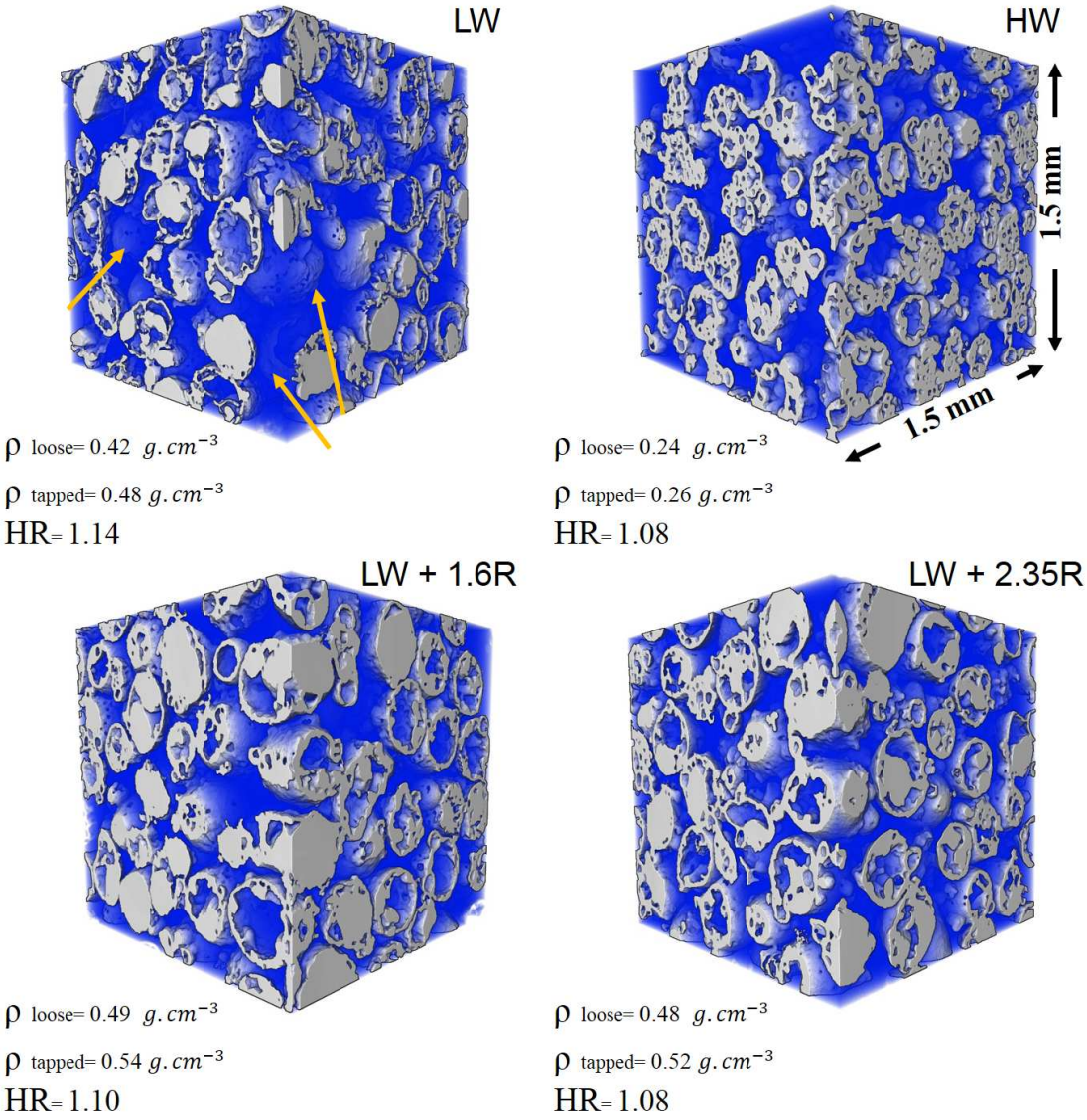

Figure 5. XRT visualization (voxel size: 2.56 µm) of the packing of spray-dried detergent powders. The 3D cubes (1.5×1.5×1.5 mm) were cropped from their original volume. The arrows highlight the presence of relatively large interstitial spaces (blue regions) within a tapped powder bed. The results of bulk density measurements, *i.e.* ρ_{loose} and ρ_{tapped}, obtained from the mechanical tapping device, and the corresponding Hausner ratios (HR) are summarized on the panels (a-d).

3.3. Surface texture and surface chemical composition

Surface composition of the granular products has been demonstrated to have a significant effect on their flow behaviour. Surface chemical composition not only influences the intra-particle forces, *e.g*. van der Waals and capillary forces, between powder particles, but also determines the micro-properties, *e.g*. stiffness and softness, in particle-surface contacts. Raman spectroscopy is known to be a convenient probe for qualitative and quantitative analysis of the concentration of molecules on the material surfaces. When Raman spectrometer is combined with a confocal microscope, it is possible to obtain detailed information regarding the chemical composition from the particle surface (Kudelski, 2008). Fig. 6a shows the Raman spectra of spray-dried detergent powders in the 400-1250 cm^{-1} region. The Raman spectra are dominated by a very sharp and intense band at ~ 990 cm^{-1} which is attributed to symmetric stretching vibrational mode (υ_1) of the free SO_4^{-2}anion with a tetragonal symmetry T_d, in the lattice of sodium sulphate crystal. Peaks corresponding to the asymmetric stretching vibrational mode (υ_3) of sodium sulphate occur at higher wavenumbers than the υ_1 mode, while the bending vibrational modes (υ_2 and υ_4) are expected at lower wave numbers (Hamilton and Menzies, 2010). For the HW powders, three sharp and distinct Raman bands at 1099, 1132 and 1150 cm^{-1} are assigned to the υ_3 mode of the sulphate in sodium sulphate crystal lattice. A doublet is seen in υ_2 region with peaks at 447 and 464 cm^{-1}, and finally, well-defined triple peaks assigned to υ_4 mode, occur between 618, 631 and 646 cm^{-1}. These well distinguished and very sharp peaks demonstrate the existence of anhydrous sodium sulphate crystals, *i.e*. thenardite, on the particle surface (Ben Mabrouk et al., 2013). The Raman peaks observed at 1047 and1191 cm^{-1} can be assigned to the symmetric and asymmetric stretching vibrations of S-O bonds in sulphonate group of LAS, which is in good agreement with the FTIR patterns reported in the literature (Wang et al., 2012, Xu and Braterman, 2003). For the HW formulations, two peak components at 1047 and 1191 cm^{-1} are very weak and appear as a shoulder.

For detergent granules produced from low-water content slurries, however; the Raman peaks at 1101, 1132 and 1150 cm^{-1}, which are assigned to the asymmetric S-O stretch of sodium sulphate crystals, are less resolved and of lower intensity (signal to noise ratio) than those of powders produced from HW slurries. On the other hand, the peaks at 1047 and 1191 cm^{-1}, assigned to asymmetric stretching vibration of S-O bonds in LAS, are noticeably stronger. In general, the Raman signal is proportional to the concentration of functional groups. These significant differences in spectral features, therefore, implies a relatively higher concentration of the surfactant on the surface of the granules produced from low-water-content slurries.

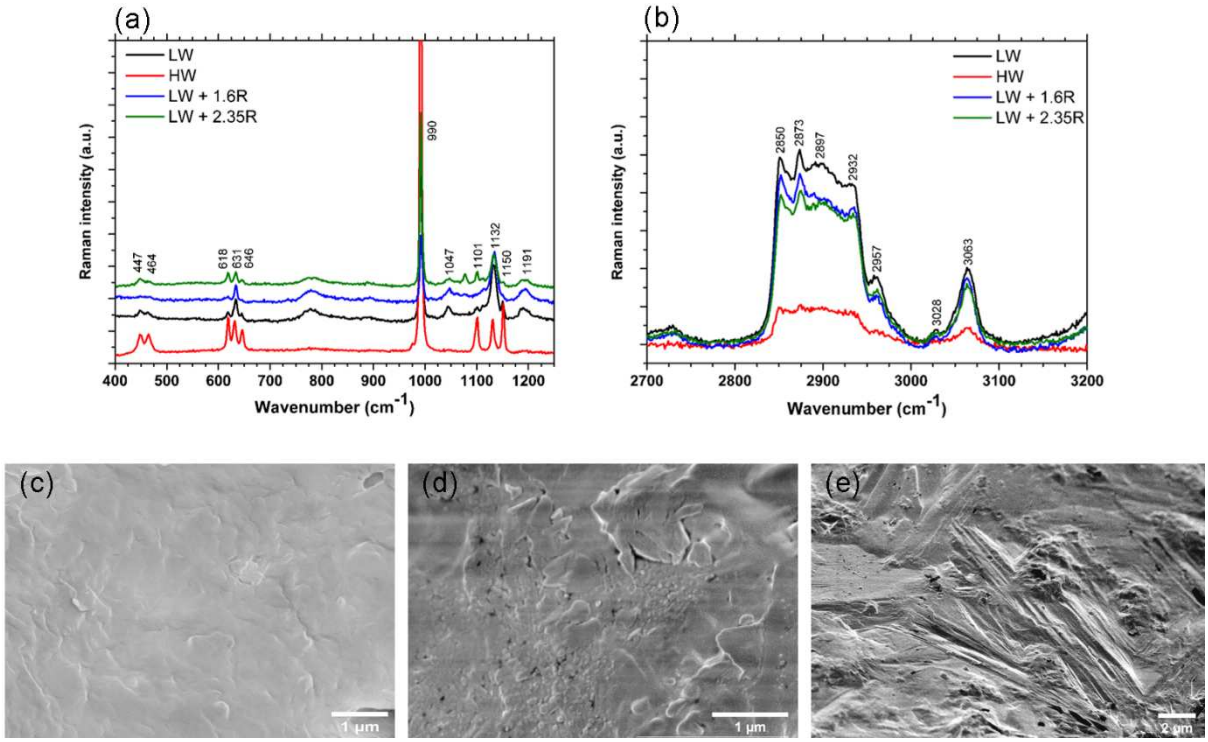

Figure 6. Surface characterization of spray-dried detergent powders: (a) Raman spectra of the detergent granules in the 400-1400 cm^{-1} region showing the intensity of the vibrational modes of S-O bonds, (b) Raman spectra in the C-H stretching region (2800-3100 cm^{-1}). (c) and (d) show SEM micrographs of the surface micro-structure of detergent granules for LW and LW + 1.6 R formulations respectively, having a relatively smooth surface. (e) shows a more crystalline surface for the HW formulation.

The C-H aliphatic stretching frequency occurs in the range of 2800-3000 cm^{-1} where the spectra are dominated by symmetric and asymmetric stretching vibratisns of methyl groups (-

CH_3) and methylene groups (-CH_2) of the alkyl chains. The peaks between 3000 and 3100 cm^{-1} are assigned to aromatic C-H stretching modes of benzene rings (Li et al., 2005, Watry and Richmond, 2000). Since LAS surfactant molecules possess a benzene ring attached to a long hydrophobic alkyl chain in their structures, the intensities of the aforementioned stretching modes in Raman spectrum can be, more specifically, used to evaluate the concentration of LAS on the granule surface. Typical Raman spectrum obtained from the detergent granules can be seen in Fig. 6b. For the LW powders, in the absence of sodium silicate, a relatively higher intensity of peaks between 2917 and 2850 cm^{-1}, signifies larger quantities of LAS surfactant on the surface. The addition of sodium silicate resulted in a noticeable reduction in intensities. This was expected since this alters the chemical composition of the surface. However, the lowest intensity was observed when the initial water content of the slurries was increased to 63 wt%.

Returning to the composition of the detergent slurries presented in Table 1, although LW and HW formulations differ in initial LAS concentration, they are estimated to have identical chemical composition upon removal of water. However, according to the Raman results, the surface of detergent powders produced from low-water content slurries appears to be richer in LAS. The reason for this can be explained by the difference in matrix composition. The higher the concentration of water, the greater is the amount of dissolved sodium sulphate within the slurry matrix. The changes of dissolved sodium sulphate-to-LAS "active matter" ratio within the liquid matrix can be subsequently reflected in the dried matrix, and hence surface composition of resulting detergent powders. Therefore, it is the increased dissolved sodium sulphate within the matrix that is mainly responsible for the observed reduction in the aliphatic C-H stretching intensity of LAS. This view can be better elucidated by examining the surface micro-structure of the detergent granules. A more crystalline surface was observed for the HW powders (Fig. 6e) as compared to those seen in the LW and LW+1.6R

powders (Fig. 6c and d). The microscopic observations of nil-silicate powders (LW) became of significant interest as viewed in conjunction with the results of confocal Raman microscopy indicating the highest intensity in the C-H aliphatic stretching region as the consequence of a greater LAS concentration. It has been reported that LAS powders are intrinsically sticky and are less free flowing (Zoller, 2004). This can potentially explain the lower flowability for these samples. Therefore, the effect of the level of LAS in the matrix on the flow behaviour of the detergent powders is twofold. On one hand the presence of LAS on the granule surface increases the cohesion of the powders. On the other hand, the higher LAS ratio to dissolved sodium sulphate within the matrix may result in more plastic surface contacts between the powder particles which consequently increases the cohesion within the powder bed.

3.4. Mechanical properties

The mean rupture strength values and Kawakita parameters obtained from the single and bulk compression tests are presented in Table 5. For the single granule compression tests, the nil-silicate detergent granules produced from low-water content slurry (LW) showed the lowest mean rupture strength. Fig. 7a shows the typical load-displacement profiles of these detergent granules. As it was mentioned earlier in the Materials and Methods section, the first sharp peak, *i.e*. the peak failure force, is used to calculate the granule strength, σ_r. In the case of LW formulations, the detergent granules begin to deform plastically under noticeably low rupture loads. Also, it can be seen that the measured load increases slowly with increasing the displacement up to the first breakage point and then decreases gently. However, the profiles for other detergent granules show an abruptly decreasing load during the first breakage, suggesting more robust granular structure.

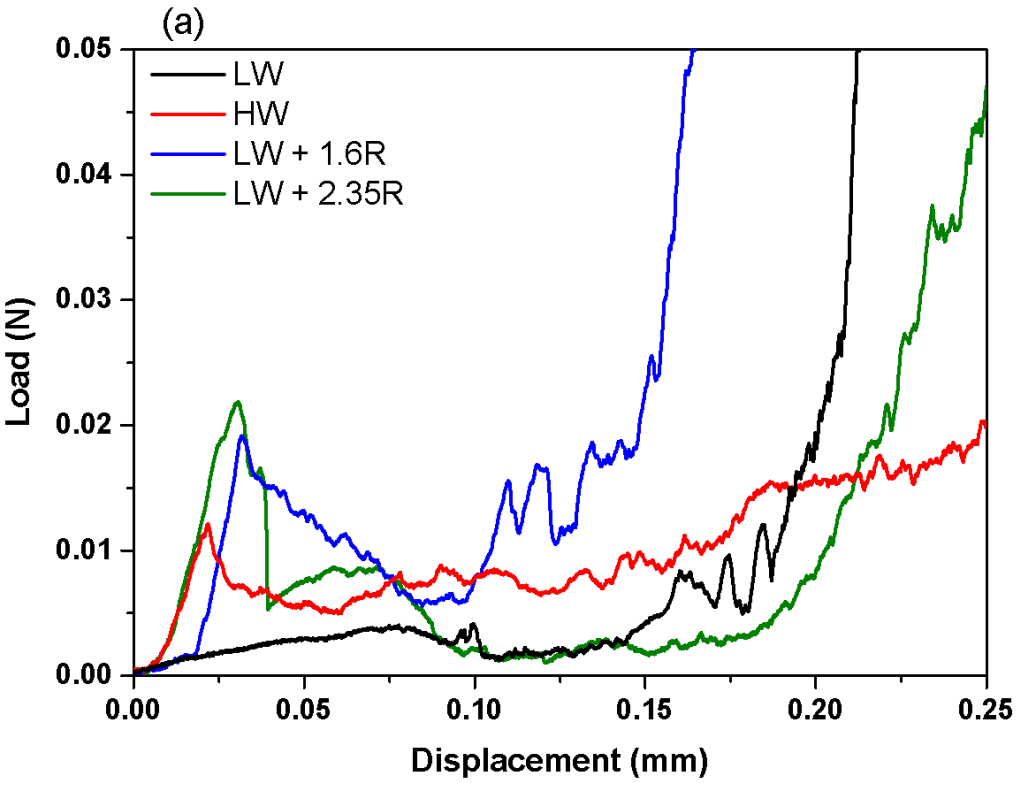
(a)
LW
HW
LW + 1.6R
LW + 2.35R
Load (N)
0.00
0.01
0.02
0.03
0.04
0.05
0.00
0.05
0.10
0.15
0.20
0.25
Displacement (mm)

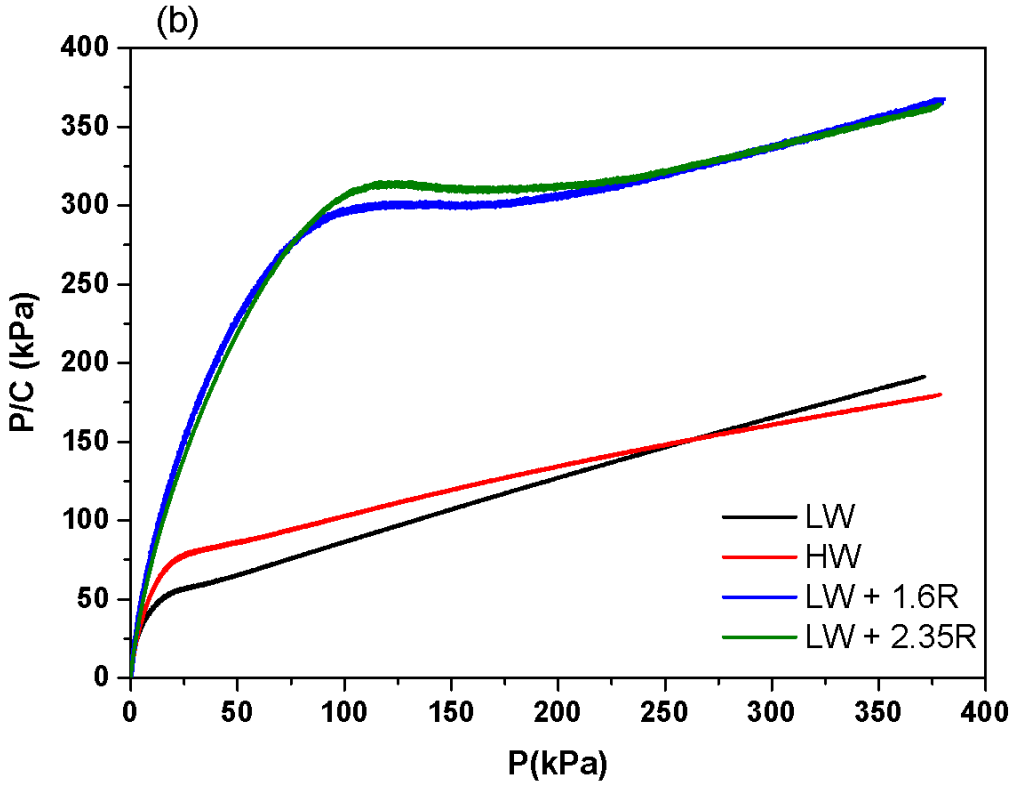
(b)
P/C (kPa)
0
50
100
150
200
250
300
350
400
0
50
100
150
200
250
300
350
400
P(kPa)
LW
HW
LW + 1.6R
LW + 2.35R

Figure. 7. Mechanical strength measurements: (a) typical force-displacement curve obtained from the single granule compression test, (b) Kawakita plots for the bulk compression of spray-dried detergent powders.

The relatively weak granular structure in LW formulation, can potentially explain the consolidation behaviour of these powders during the pre-shearing stage of shear cell test measurements (Fig. 4b). A noticeably large displacement, which is a measure of the extent of strain within the powder bed, was partially attributed to plastic deformation. In general, the softer the particle contacts, the greater are the plastic deformation around the contacts and, hence, the poorer is the powder flow (Tomas, 2004b). Therefore, it was a relatively weaker particle strength that was responsible for the poor powder flow behaviour. The increased water content of the detergent slurry used to manufacture the HW formulation, leads to a distinct change in the breakage behaviour and a significant increase in the mechanical strength of the resulting granules. This can be attributed to the increased level of sodium sulphate in the matrix.

The mechanical strength of the powders was increased significantly by the addition of sodium silicates to the detergent slurries, according to the Tukey's multiple comparison test (Table 5). This was expected since sodium silicate is long established as effective binder in spray dried detergent formulations and many other applications (Goberis and Stonis, 2004, Yang et al., 2008). Alkaline silicate solutions are colloidal dispersions of monomeric and polymeric anions, upon drying, the removal of water from the interstitial spaces causes aggregates to come into close proximity until they form a rigid glass (Roggendorf et al., 2015). The formation of this glassy binder can therefore impart a rigid characteristic on the granule microstructure. The addition of sodium silicate with SiO_2:Na_2O molar ratio of 1.6 was very effective at increasing the mean rupture strength of the granules. However, the

largest mean rupture strength was observed once the molar ratio was increased to 2.35. This can be explained by both the higher absolute level of SiO_2, due to the higher ratio, and an increased degree of silicate polymerisation, due to the lower Na_2O content, which can form a mechanically stronger dried structure (Böschel et al., 2003, Yang et al., 2008). It should also be noted that the higher ratio can also lead to lower particle dissolution rates and decreases the solubility of the powders.

Table 5. Average values with standard deviations for the parameters of bulk compression model, and the granule rupture strength derived from the single compression test.

Sample	Single particle compression	Kawakita and Lüdde	
	σ_r, *kPa*	*a*	*1/b, kPa*
LW	27.29±9.42 [a]	2.69±0.06	135±27
HW	72.75±25.28 [a]	3.37±0.56	264±59
LW + 1.6R	239.44±83.51 [b]	2.68±0.03	576±31
LW + 2.35R	262.34±77.50 [b]	2.80±0.04	674±64

Note: Within the Single particle compression column, the mean values labelled with same letter were not significantly different (Tukey's test, α=0.05). More details about the statistical tests are presented in Appendix.

The fitting of the experimental bulk compression data into Kawakita model provided a good understanding of the consolidation mechanisms, *e.g*. particle rearrangement and plastic deformation, as well as overall mechanical properties, *e.g*. yield strength, of the powders. Typical Kawakita plots for spray-dried powers are presented in Fig. 7b. In all cases the plots show a curved profile at initial compressive pressures, and a linear region can be observed at larger compacting pressures. In general, the initial curved region is mainly attributed to granule sliding and rearrangment at the beginning of compaction process. For the nil-silicate samples produced from low-water content slurries (LW), this non-linear region is limited to a

noticeably small compressive pressure range (P < 25 kPa), which suggests that compaction of theses powders mainly occurs through plastic deformation (Arifvianto et al., 2015).

From Table 5 the lowest value of Kwakita parameter 1/b indicates that these powders possess the least resistence against compression. For the HW formulation , the Kawakita plots of the resulting powders tend to bend at a slightly larger compressive pressure around ~ 50 kPa, suggessting a relatively stronger powder bed structure against compression. However, the addition of sodium silicate resulted in the plots having a more pronounced curve in a larger range of pressure up to ~125 kPa, which suggests that particle rearrangement plays a significant role in consolidation behaviour of these powders. This yielded larger 1/b values comparing to the nil-silicate samples. Regarding the Kawakita parameter *a*, the values were similar for the samples produced from all the low-water content slurries. However, detergent powders produced from high-water content slurry showed the largest values of physical constant *a*, indicating a higher degree of compression at an infinite compression pressure (Nordström et al., 2009). This is a consequence of the lower bulk density, and high porosity of the HW formulation. The increased slurry water content leading to a significant change in internal particle structure and a higher intraparticle porosity. From Fig. 5 it can be seen that these powders possess the lowest bulk density (ρ_{loose}=0.24 g.cm^3), about half that of the LW powders.

4. Conclusion

The flow behaviour of four model formulations was investigated using a shear cell tester. Careful analysis of these results, complemented by detailed analysis of the micro-structure and mechanical characteristics of the formulations showed that the powder flow behaviour was governed by particle robustness and micro-structure, which are both governed by matrix composition. Particle morphology was not seen to play a significant role.

The LW powder made from low water-content slurries was the most cohesive and had a tendency to form a structurally loose powder bed with considerable intra-granular porosity. The flow behaviour of these powders; however, noticeably improved once the initial water content of the slurries increased to 63 wt%. The poor flow characteristics of LW powders were attributed to the formation of a mechanically soft matrix phase which contained a larger quantity of LAS surfactant, compared to the HW powders. In other words, both LW and HW powders have virtually identical chemical compositions; however, their matrix composition is significantly different. The increased water content of the slurry, results in a greater ratio of dissolved sodium sulphate to LAS phase within the matrix, which was reflected in the surface composition and texture of the HW granules, leading to the increased mechanical strength of the granules.

The addition of sodium silicate with SiO_2:Na_2O molar ratio of 1.6 to the LW formulations, noticeably improved their flow behaviour which, once again, was attributed to the increased micro-structural strength of the detergent granules. The silicate is thought to form a glassy continuum linking sulphate crystals and surfactant domains, which consequently increases the apparent granule strength. Also, the detergent powders became easy-flowing ($ff_c < 10$) once sodium silicate with the SiO_2:Na_2O molar ratio of 2.35 was added to the LW formulations, which was attributed to the increased level of SiO_2 and increased mechanical strength of the silicate structure formed.

In this study, the critical role of the matrix phase in determining the mechanical properties and flow behaviour of spray-dried detergent powders was particularly highlighted. The addition of binders and even simple changes such as the amount of water in slurry can significantly change the nature of the surface micro-structure and hence the flow behaviour of detergent powders. The findings of this study can help engineers and formulation scientists, optimise processes and formulations in detergent industries.

Acknowledgement

The authors would like to thank the Advanced Manufacturing Supply Chain Initiative (AMSCI) [grant number 31587, 233189] for funding the project. AMSCI is a government supply chain fund which is helping to rebuild British manufacturing processes. We also acknowledge the input of Joel Caragay and Paul Gould of Procter and Gamble for production of materials and their support throughout the project.

References

ARIFVIANTO, B., LEEFLANG, M. A. & ZHOU, J. 2015. The compression behaviors of titanium/carbamide powder mixtures in the preparation of biomedical titanium scaffolds with the space holder method. *Powder Technology,* 284**,** 112-121.

BARJAT, H., CHECKLEY, S., CHITU, T., DAWSON, N., FARSHCHI, A., FERREIRA, A., GAMBLE, J., LEANE, M., MITCHELL, A., MORRIS, C., PITT, K., STOREY, R., TAHIR, F. & TOBYN, M. 2020. Demonstration of the Feasibility of Predicting the Flow of Pharmaceutically Relevant Powders from Particle and Bulk Physical Properties. *Journal of Pharmaceutical Innovation*.

BEN MABROUK, K., KAUFFMANN, T. H., AROUI, H. & FONTANA, M. D. 2013. Raman study of cation effect on sulfate vibration modes in solid state and in aqueous solutions. *Journal of Raman Spectroscopy,* 44**,** 1603-1608.

BOEREFIJN, R., DONTULA, P.-R. & KOHLUS, R. 2007. Chapter 14 Detergent granulation. *In:* A.D. SALMAN, M. J. H. & SEVILLE, J. P. K. (eds.) *Handbook of Powder Technology.* Elsevier Science B.V.

BÖSCHEL, D., JANICH, M. & ROGGENDORF, H. 2003. Size distribution of colloidal silica in sodium silicate solutions investigated by dynamic light scattering and viscosity measurements. *Journal of Colloid and Interface Science,* 267**,** 360-368.

FARSHCHI, A., HASSANPOUR, A. & BAYLY, A. E. 2019a. The structure of spray-dried detergent powders. *Powder Technology,* 355**,** 738-754.

FARSHCHI, A., HASSANPOUR, A., ETTELAIE, R. & BAYLY, A. E. 2019b. Evolution of surface micro-structure and moisture sorption characteristics of spray-dried detergent powders. *Journal of Colloid and Interface Science,* 551**,** 283-296.

FARSHCHI, A., SADEGHPOUR, A., RAPPOLT, M., TANTAWY, H., CARAGAY, J., ROBLES, E. S. J., HASSANPOUR, A. & BAYLY, A. 2021. Liquid crystalline phases of linear alkylbenzene sulphonate in spray-dried detergent powders studied by small-angle X-ray scattering, TEM, and ATR-IR spectroscopy. *Colloids and Surfaces A: Physicochemical and Engineering Aspects,* 614**,** 126130.

FITZPATRICK, J. J., BARRINGER, S. A. & IQBAL, T. 2004a. Flow property measurement of food powders and sensitivity of Jenike's hopper design methodology to the measured values. *Journal of Food Engineering,* 61**,** 399-405.

FITZPATRICK, J. J., IQBAL, T., DELANEY, C., TWOMEY, T. & KEOGH, M. K. 2004b. Effect of powder properties and storage conditions on the flowability of milk powders with different fat contents. *Journal of Food Engineering,* 64**,** 435-444.

GAMBLE, J. F., FERREIRA, A. P., TOBYN, M., DIMEMMO, L., MARTIN, K., MATHIAS, N., SCHILD, R., VIG, B., BAUMANN, J. M., PARKS, S. & ASHTON, M. 2014. Application of imaging based tools for the characterisation of hollow spray dried amorphous dispersion particles. *International Journal of Pharmaceutics,* 465**,** 210-217.

GOBERIS, S. & STONIS, R. 2004. Advantageous features of sodium silicate as the plasticizer for low-cement refractory castables. *Refractories and Industrial Ceramics,* 45**,** 446-449.

HAMILTON, A. & MENZIES, R. I. 2010. Raman spectra of mirabilite, Na2SO4·10H2O and the rediscovered metastable heptahydrate, Na2SO4·7H2O. *Journal of Raman Spectroscopy,* 41**,** 1014-1020.

HAYES, G. D. 1987. *Food engineering data handbook,* Harlow, Longman Scientific & Technical.

HINTZ, W., ANTONYUK, S., SCHUBERT, W., EBENAU, B., HAACK, A. & TOMAS, J. 2008. Determination of Physical Properties of Fine Particles, Nanoparticles and Particle Beds. *Modern Drying Technology.* Wiley-VCH Verlag GmbH & Co. KGaA.

JENIKE, A. W. 1967. Quantitative design of mass-flow bins. *Powder Technology,* 1**,** 237-244.

KAWAKITA, K. & LÜDDE, K.-H. 1971. Some considerations on powder compression equations. *Powder Technology,* 4**,** 61-68.

KEELEY, C. T. 1983. Sodium silicate: The key ingredient in detergent agglomeration. *Journal of the American Oil Chemists' Society,* 60**,** 1370-1372.

KHOMANE, K. S., MORE, P. K., RAGHAVENDRA, G. & BANSAL, A. K. 2013. Molecular Understanding of the Compaction Behavior of Indomethacin Polymorphs. *Molecular Pharmaceutics,* 10**,** 631-639.

KUDELSKI, A. 2008. Analytical applications of Raman spectroscopy. *Talanta,* 76**,** 1-8.

LI, L., MIZUHATA, M. & DEKI, S. 2005. Preparation and characterization of alkyl sulfate and alkylbenzene sulfonate surfactants/TiO2 hybrid thin films by the liquid phase deposition (LPD) method. *Applied Surface Science,* 239**,** 292-301.

LI, Q., RUDOLPH, V., WEIGL, B. & EARL, A. 2004. Interparticle van der Waals force in powder flowability and compactibility. *International Journal of Pharmaceutics,* 280**,** 77-93.

LIU, L. X., MARZIANO, I., BENTHAM, A. C., LITSTER, J. D., E.T.WHITE & HOWES, T. 2008. Effect of particle properties on the flowability of ibuprofen powders. *International Journal of Pharmaceutics,* 362**,** 109-117.

MARSHALL, C. P. & OLCOTT MARSHALL, A. 2013. Raman hyperspectral imaging of microfossils: potential pitfalls. *Astrobiology,* 13**,** 920-931.

MUIR, D. D. 2007. Encapsulated and Powdered Foods. *International Journal of Dairy Technology,* 60**,** 61-61.

NORDSTRÖM, J. & ALDERBORN, G. 2011. Degree of compression as a potential process control tool of tablet tensile strength. *Pharmaceutical Development and Technology,* 16**,** 599-608.

NORDSTRÖM, J., KLEVAN, I. & ALDERBORN, G. 2009. A particle rearrangement index based on the Kawakita powder compression equation. *Journal of Pharmaceutical Sciences,* 98**,** 1053-1063.

PASHA, M., DOGBE, S., HARE, C., HASSANPOUR, A. & GHADIRI, M. 2014. A linear model of elasto-plastic and adhesive contact deformation. *Granular Matter,* 16**,** 151-162.

POSZYTEK, K. 2005. *Wheat flour flowability as affected by water activity, storage time and consolidation*, Institute of Agrophysics.

ROGGENDORF, H., BÖSCHEL, D. & TREMPLER, J. 2001. Structural evolution of sodium silicate solutions dried to amorphous solids. *Journal of Non-Crystalline Solids,* 293-295**,** 752-757.

ROGGENDORF, H., FISCHER, M., ROTH, R. & GODEHARDT, R. 2015. Influence of Temperature and Water Vapour Pressure on Drying Kinetics and Colloidal Microstructure of Dried Sodium Water Glass. *Advances in Chemical Engineering and Science,* Vol.05No.01**,** 11.

SAMIMI, A., HASSANPOUR, A. & GHADIRI, M. 2005. Single and bulk compressions of soft granules: Experimental study and DEM evaluation. *Chemical Engineering Science,* 60**,** 3993-4004.

SCHUBERT, H. 1987. Food particle technology. Part I: Properties of particles and particulate food systems. *Journal of Food Engineering,* 6**,** 1-32.

SCHULZE, D. 2007. *Powders and bulk solids: behavior, characterization, storage and flow*, Springer Science & Business Media.

TOGNONVI, M. T., MASSIOT, D., LECOMTE, A., ROSSIGNOL, S. & BONNET, J.-P. 2010. Identification of solvated species present in concentrated and dilute sodium silicate solutions by combined 29Si NMR and SAXS studies. *Journal of Colloid and Interface Science,* 352**,** 309-315.

TOMAS, J. 2004a. Fundamentals of cohesive powder consolidation and flow. *Granular Matter,* 6**,** 75-86.

TOMAS, J. 2004b. Product Design of Cohesive Powders – Mechanical Properties, Compression and Flow Behavior. *Chemical Engineering & Technology,* 27**,** 605-618.

ULUSOY, U. & KURSUN, I. 2011. Comparison of different 2D image analysis measurement techniques for the shape of talc particles produced by different media milling. *Minerals Engineering,* 24**,** 91-97.

WANG, D.-Y., DAS, A., LEUTERITZ, A., MAHALING, R. N., JEHNICHEN, D., WAGENKNECHT, U. & HEINRICH, G. 2012. Structural characteristics and flammability of fire retarding EPDM/layered double hydroxide (LDH) nanocomposites. *RSC Advances,* 2**,** 3927-3933.

WATRY, M. R. & RICHMOND, G. L. 2000. Comparison of the Adsorption of Linear Alkanesulfonate and Linear Alkylbenzenesulfonate Surfactants at Liquid Interfaces. *Journal of the American Chemical Society,* 122**,** 875-883.

XU, Z. P. & BRATERMAN, P. S. 2003. High affinity of dodecylbenzene sulfonate for layered double hydroxide and resulting morphological changes. *Journal of Materials Chemistry,* 13**,** 268-273.

YANG, X., ZHU, W. & YANG, Q. 2008. The Viscosity Properties of Sodium Silicate Solutions. *Journal of Solution Chemistry,* 37**,** 73-83.

ZHOU, D. & QIU, Y. 2010. Understanding material properties in pharmaceutical product development and manufacturing: Powder flow and mechanical properties. *Journal of Validation Technology,* 16**,** 65.

ZOLLER, U. 2004. *Handbook of detergents, Part B: Environmental impact*, CRC Press.

ZOLLER, U. & SOSIS, P. 2008. *Handbook of detergents, part F: Production*, CRC Press.